Electronic Supplementary Material (ESI) for Chemical Science.

Electronic supplementary information

Uncovering an oxide ion substitution for the OH^- + CH_3F reaction

Domonkos A. Tasi* and Gábor Czakó*

MTA-SZTE Lendület Computational Reaction Dynamics Research Group, Interdisciplinary Excellence Centre
and Department of Physical Chemistry and Materials Science, Institute of Chemistry, University of Szeged,
Rerrich Béla tér 1, Szeged H-6720, Hungary

* dtasi@chem.u-szeged.hu (D.A.T.) and gczako@chem.u-szeged.hu (G.C.)

Computational methods

Benchmark *ab initio* thermochemistry

The stationary points of the $OH^{-} + CH_3F$ reaction are searched using the second-order Møller–Plesset perturbation theory (MP2)[1] with the aug-cc-pVDZ basis set.[2] Then the explicitly-correlated coupled-cluster singles, doubles, and perturbative triples (CCSD(T)-F12b) method[3] is employed with the aug-cc-pVDZ and aug-cc-pVTZ basis sets in order to improve the accuracy of the structures, energies and frequencies of the stationary points. The benchmark classical energies are computed at the CCSD(T)-F12b/aug-cc-pVTZ geometries using the CCSD(T)-F12b method with aug-cc-pVQZ basis set, as well as considering: (a) post-CCSD(T) correlation effects up to CCSDT(Q) and (b) core correlation effects. These single-point computations are performed using (a) the CCSD(T),[4] CCSDT,[5] and CCSDT(Q)[6] methods with the aug-cc-pVDZ basis set and (b) the CCSD(T) method with the aug-cc-pwCVTZ basis set applying both frozen-core (FC) and all-electron (AE) approaches. As for the FC calculations, the valence electrons are correlated only, for the AE approach, the $1s^2$ (C, O, F) electrons are also correlated. Thus, the benchmark classical (adiabatic) relative energies of the stationary points are computed as:

$$\Delta E(\text{CCSD(T)-F12b/aug-cc-pVQZ}) + \delta[\text{CCSDT}] + \delta[\text{CCSDT(Q)}] + \Delta\text{core} \ (+\ \Delta\text{ZPE}), \quad (\text{S1})$$

where

$$\delta[\text{CCSDT}] = \Delta E(\text{CCSDT/aug-cc-pVDZ}) - \Delta E(\text{CCSD(T)/aug-cc-pVDZ}), \quad (\text{S2})$$

$$\delta[\text{CCSDT(Q)}] = \Delta E(\text{CCSDT(Q)/aug-cc-pVDZ}) - \Delta E(\text{CCSDT/aug-cc-pVDZ}) \quad (\text{S3})$$

and

$$\Delta\text{core} = \Delta E(\text{AE-CCSD(T)/aug-cc-pwCVTZ}) - \Delta E(\text{FC-CCSD(T)/aug-cc-pwCVTZ}) \quad (\text{S4})$$

and ΔZPE is the harmonic zero-point energy correction obtained at the CCSD(T)-F12b/aug-cc-pVTZ level of theory.

The benchmark relative energies of the stationary points are adapted from our previous study of the title reaction,[7] the FSTS2, PostHMIN1′ and PostHMIN2 are newly characterized in this work. All the *ab initio* computations are carried out with the MOLPRO program package,[8] except for CCSDT and CCSDT(Q), in these cases the MRCC program[9,10] is utilized, interfaced to MOLPRO.

Development of the potential energy surface

For the development of the global analytical *ab initio* PES of the OH^- + CH_3F reaction the same procedure is utilized as in the case of the OH^- + CH_3I reaction.[11] The PES development is performed with the ROBOSURFER program package[12] at the MP2/aug-cc-pVDZ level of theory. The first step is to generate an initial dataset (14072 structures) by two methods: modifying the geometries of the stationary points randomly and changing the positions between the fragments of the reactants or products within 2.0 to 10.0 Å from each other. Then, this dataset is used to start the ROBOSURFER program, which adds the remaining points by iterative selection of the energies of the new geometries derived from quasiclassical trajectory (QCT) simulations. Performing 11, 85, 114, 85, 80, 55, 50, 50, 55, 70 iterations at 1, 5, 10, 20, 30, 40, 50, 60, 70 and 80 kcal mol^{-1} collision energies (E_{coll}) in order, the dataset contains 50434 energy points. In every iteration 24 trajectories are run with different impact parameters (b): 0.0, 0.5, 1.0, 1.5, 2.0, 2.5, 4.0, and 9.0 bohr (3 trajectories at each b). The energy window has a hard upper limit of 220 kcal/mol relative to the global minimum optimized at MP2/aug-cc-pVDZ and no lower limit. The targeted PES accuracy is adjusted to 0.5 kcal mol^{-1}, and the full accuracy limit is set to 95.2 kcal/mol relative to free reactants. The latter energy value is set by considering our previous study on the OH^- + CH_3I reaction.[11] The HOLEBUSTER subprogram is not utilized for PES development. The permutationally invariant polynomial approach is used for fitting the PES applying a fifth-order polynomial expansion of Morse-like variables, $\exp(-r_{ij}/a)$, where r_{ij} are the inter-atomic distances and a = 3 bohr.[13,14] The 4693 polynomial coefficients of the fit are determined by a weighted linear least-squares fit applying the weight function of $E_0/(E + E_0)\times E_1/(E + E_1)$, where E_0 = 94 kcal/mol, E_1 = 314 kcal/mol, and E is the energy relative to the global minimum. The DGELSY and DGELS standard LAPACK subroutines are applied to solve the linear least-squares problems. Similar to the OH^- + CH_3I reaction,[11] at certain geometries the gold-standard CCSD(T) breaks down providing too negative energies, therefore to avoid this problem, the energy points are recalculated at the following composite level of theory:[11,15]

$$\text{CCSD-F12b/aug-cc-pVTZ} + \text{BCCD(T)/aug-cc-pVDZ} - \text{BCCD/aug-cc-pVDZ}. \qquad \text{(S5)}$$

Moreover, we add 1002 composite *ab initio* energy points to improve the region of the PES, which leads to the HF + CH_3O^- products. The final PES contains 51433 energy points (convergence problems are found only in three cases) and the root-mean-squared fitting errors are: 0.83 kcal mol^{-1}, 1.69 kcal mol^{-1}, and 2.54 kcal mol^{-1} for the energy ranges 0–94 kcal mol^{-1}, 94–188 kcal mol^{-1} and 188–471 kcal mol^{-1}, respectively.

Quasiclassical trajectory calculations

QCT computations are carried out for the OH^{-} + CH_3F reaction at ten E_{coll}: 5, 10, 15, 20, 30, 40, 50, 60, 70 and 80 kcal mol^{-1} using a time step of 0.0726 fs. The ground vibrational states of OH^{-} and CH_3F are prepared by standard normal-mode sampling and the rotational angular momenta are set to 0. The initial distance of the reactants is 25 bohr with a given b, and the initial spatial orientation of the reactants is randomly sampled. At each b, 5000 trajectories are run and b is scanned with the step size of 0.5 bohr from 0 to b_{max}, where the probability of the reaction becomes 0. Each trajectory is propagated until the largest interatomic separation becomes larger by 1 bohr than the largest initial one. The cross sections (σ) are defined by a b-weighted integration of the opacity functions ($P(b)$, reaction probabilities as a function of b) as

$$\sigma = 2\pi \int_0^{b_{\max}} P(b) b \mathrm{d}b, \tag{S6}$$

which expression is determined by numerical integration using the trapezoidal rule. The scattering angle (θ) is the angle of the relative velocity vectors of the products and the reactants. According to the conventional agreement, cos (θ) = −1 corresponds to the backward scattering. For the oxide ion substitution, in case the velocity vectors of OH^{-} and HF display a 180° angle, backward scattering takes place. The distributions of this scattering angle are obtained by binning the cosine of the angle into 10 equidistant bins from −1 to 1. The identification of the S_N2 reaction, which does not avoid the $CH_3OH\cdots F^{-}$ deep well (PostHMIN1), is based on a similar method used for the numerical separation of the front-side attack and double-inversion mechanisms.[16] We follow the relevant atomic distances (C–F, C–O and the corresponding O–H and F–H) backwards from the end of the reactive S_N2 trajectories, and we assign the reaction paths to PostHMIN1 formation if the following conditions hold: Hydroxyl-H−F distance is less than 1.8 Å *and* hydroxyl-H−O distance is less than 2.5 Å *and* the C−O distance is less than the C−F distance.

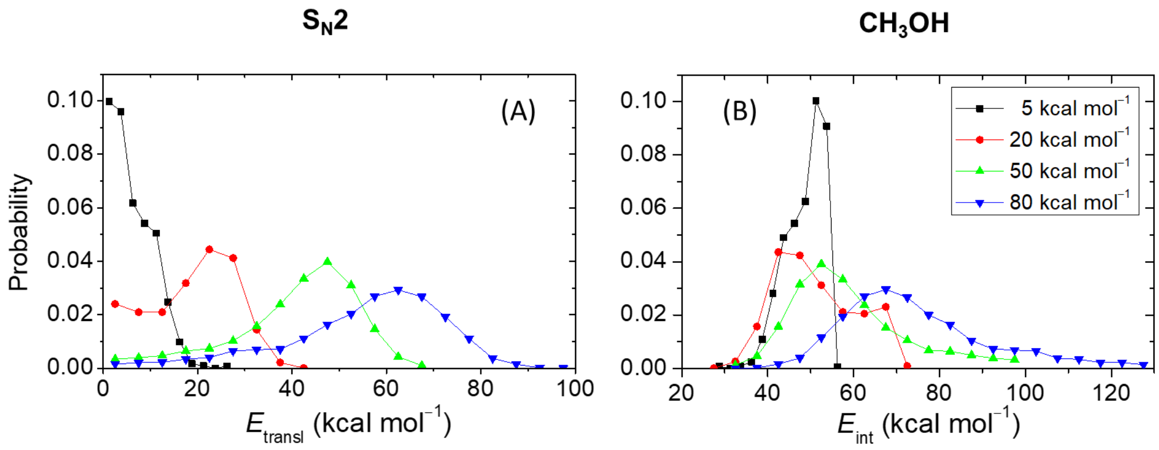

Figure S1. (A) Relative translational energy distributions of the products, and (B) internal energy distributions of the CH_3OH product at different collision energies for the $OH^{-} + CH_3F \rightarrow F^{-} + CH_3OH$ reaction.

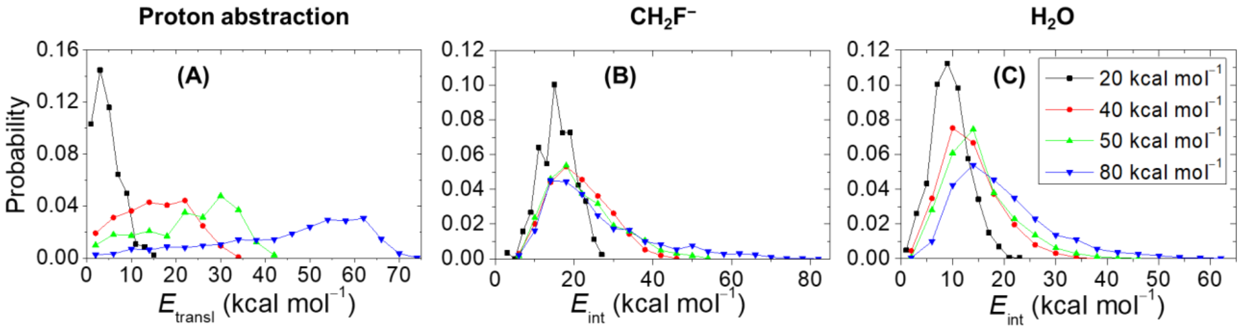

Figure S2. (A) Relative translational energy distributions of the products, and internal energy distributions of the (B) CH_2F^- and (C) H_2O products at different collision energies for the OH^- + CH_3F → CH_2F^- + H_2O reaction.

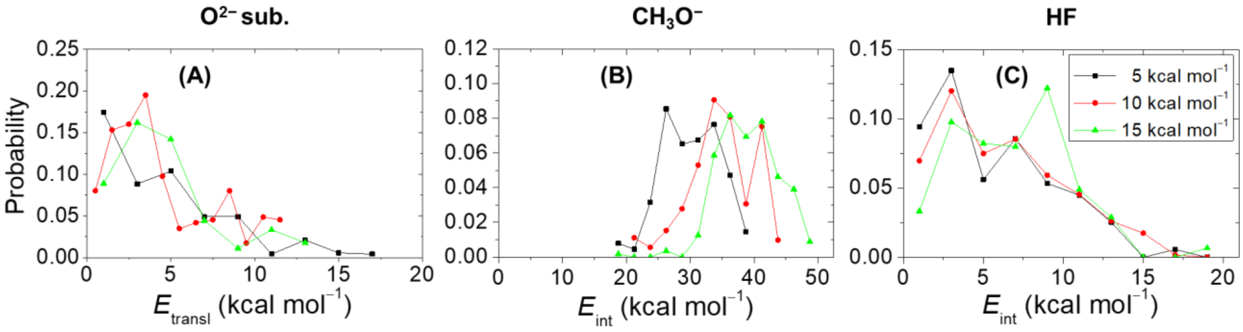

Figure S3. (A) Relative translational energy distributions of the products, and internal energy distributions of the (B) CH_3O^- and (C) HF products at different collision energies for the $OH^- + CH_3F \rightarrow CH_3O^- + HF$ reaction.

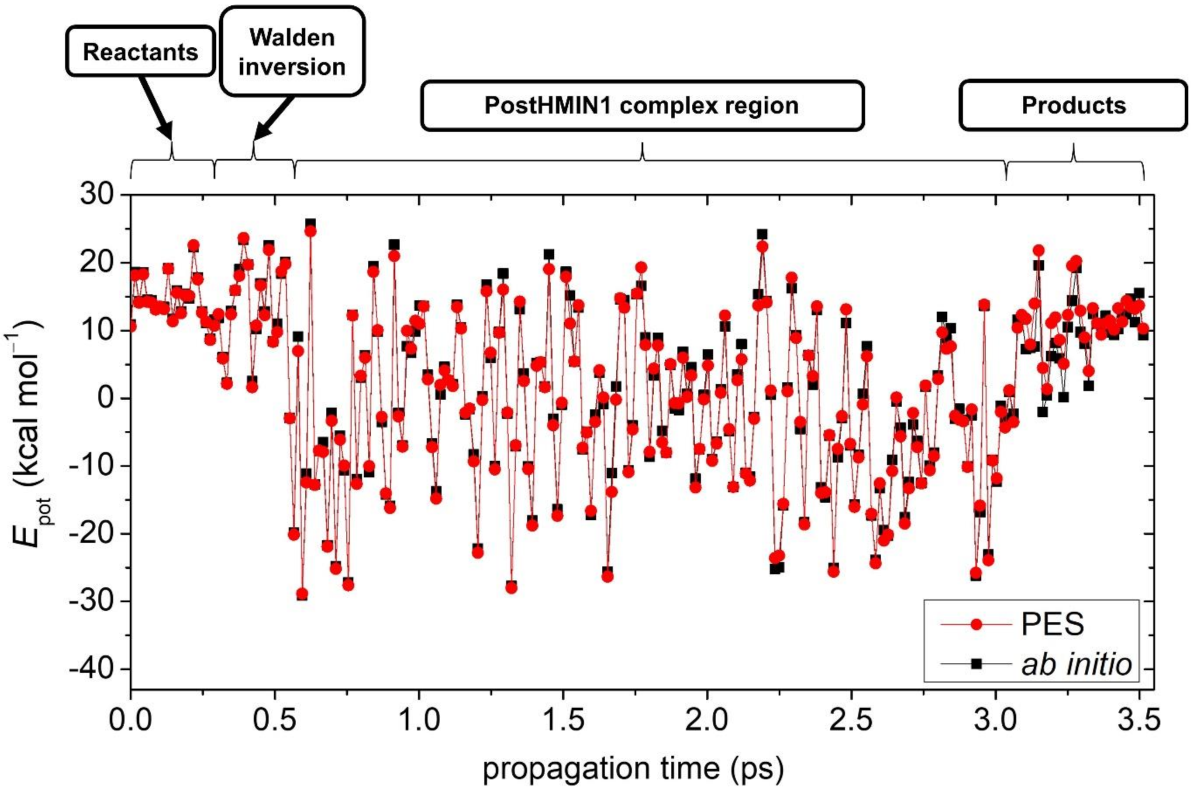

Figure S4. A representative dynamics simulation of the oxide ion substitution for the OH^{-} + CH_3F reaction at collision energy of 10 kcal mol^{-1}, where the direct *ab initio* potential energies are compared with the fitted PES values, relative to OH^{-}(eq) + CH_3F(eq), as a function of time. The *ab initio* energies are obtained at the CCSD-F12b/aug-cc-pVTZ + BCCD(T)/aug-cc-pVDZ − BCCD/aug-cc-pVDZ composite level of theory and the PES values correspond to the present analytical fitted composite PES.

Table S1. The average time (ps) that the trajectories trap into the postHMIN1 complex well at b = 0 – 3 and E_{coll} = 5, 10, 15 and 20 kcal/mol for the $OH^{-} + CH_3F \rightarrow CH_3O^{-} + HF$ reaction.[a]

***b* (bohr)**	***E*coll (kcal/mol)**			
	5	**10**	**15**	**20**
0.0	2.78	3.36	1.87	1.09
0.5	2.23	2.02	0.76	1.25
1.0	5.11	3.38	2.38	2.96
1.5	5.28	1.44	1.63	1.88
2.0	1.33	2.78	1.30	1.37
2.5	5.29	3.10	1.24	0.64
3.0	3.53	1.56	0.91	2.01

[a] For the evaluation of the lifetime of the PostHMIN1 complex we follow the relevant atomic distances (C–F, C–O and the corresponding O–H and F–H) from the beginning of the oxide anion substitution, and we assign the PostHMIN1 complex at each time step of 0.726 fs if the following conditions hold: Hydroxyl-H−F distance is less than 2.5 Å *and* hydroxyl-H−O distance is less than 2.25 Å *and* the C−O distance is less than the C−F distance *and* hydroxyl-H−F distance is not the longest H−F distance *and* hydroxyl-H−F distance is not greater by 0.3 Å than the shortest H−F distance.

Table S2. The ratio (%) of the integral cross sections of each pathway [S_N2 (*via* PostHMIN1, retention and inversion), proton abstraction, oxide anion substitution (with soft and hard ZPE-constraints) and proton exchange] for the OH^- + CH_3F reaction at different collision energies.

E_{coll} (kcal/mol)	S_N2[a]	S_N2 via PostHMIN1	S_N2 inv.	S_N2 ret.	Proton abs.[a]	O^{2-} sub.[a]	O^{2-} sub. soft[b]	O^{2-} sub. hard[c]	Proton exchange[a]
5	56.70	16.62	55.58	0.02	1.76	2.14	1.50	0.20	39.40
10	89.51	12.44	89.25	0.03	2.62	1.55	1.36	0.30	6.32
15	88.86	9.59	88.59	0.00	5.53	1.51	1.50	0.38	4.10
20	79.67	5.67	79.48	0.00	15.76	0.78	0.78	0.31	3.79
30	60.77	1.41	60.66	0.00	37.57	0.19	0.19	0.02	1.47
40	57.80	0.44	57.78	0.00	41.50	0.11	0.11	0.02	0.59
50	62.08	0.19	62.04	0.03	37.73	0.01	0.01	0.00	0.18
60	61.30	0.24	61.07	0.24	38.58	0.02	0.02	0.02	0.10
70	62.21	0.68	60.94	1.26	37.70	0.04	0.04	0.00	0.05
80	65.23	1.37	62.39	2.83	34.70	0.03	0.03	0.01	0.05

[a] 100% = $ICS_{S_N2} + ICS_{\text{Proton abs.}} + ICS_{O^{2-}\text{ sub.}} + ICS_{\text{Proton exchange}}$

[b] Those trajectories are rejected, where the sum of the classical vibrational energy of the CH_3O^- product and the internal energy of the HF product is smaller than the sum of the ZPE of CH_3O^- on the present PES and the ZPE corresponding to actual rotational state of HF.

[c] Those trajectories are rejected, where the classical vibrational energy of the CH_3O^- product is smaller than its ZPE on the present PES and the internal energy of the HF product is also smaller than its ZPE corresponding to its actual rotational state.

Additional files

Supplementary movies

Representative trajectories of (1) S_N2 inversion, (2) S_N2 inversion via PostHMIN1, (3) S_N2 double inversion, (4) proton exchange, (5) and (6) oxide anion substitution (complete and relevant part) at E_{coll} = 10 kcal mol^{-1} as well as (7) proton abstraction and (8) S_N2 front-side attack at E_{coll} = 60 kcal mol^{-1} for the OH^{-} + CH_3F reaction.

Cartesian coordinates and energies

Benchmark Cartesian coordinates (Å) and energies (E_h) of the stationary points for the OH^{-} + CH_3F reaction.

References

1 C. Møller and M. S. Plesset, *Phys. Rev.*, 1934, **46**, 618.

2 T. H. Dunning, *J. Chem. Phys.*, 1989, **90**, 1007.

3 T. B. Adler, G. Knizia and H. J. Werner, *J. Chem. Phys.*, 2007, **127**, 221106.

4 K. Raghavachari, G. W. Trucks, J. A. Pople and M. Head-Gordon, *Chem. Phys. Lett.*, 1989, **157**, 479.

5 J. Noga and R. J. Bartlett, *J. Chem. Phys.*, 1986, **86**, 7041.

6 M. Kállay and J. Gauss, *J. Chem. Phys.*, 2005, **123**, 214105.

7 D. A. Tasi, Z. Fábián and G. Czakó, *J. Phys. Chem. A,* 2018, **122**, 5773.

8 H.-J. Werner, P. J. Knowles, G. Knizia, F. R. Manby and M. Schütz, *et al*, MOLPRO, version 2015.1, a package of ab initio programs, see http://www.molpro.net.

9 M. Kállay, P. R. Nagy, D. Mester, Z. Rolik, G. Samu, J. Csontos, J. Csóka, P. B. Szabó, L. Gyevi-Nagy, B. Hégely, I. Ladjánszki, L. Szegedy, B. Ladóczki, K. Petrov, M. Farkas, P. D. Mezei and Á. Ganyecz, *J. Chem. Phys.*, 2020, **152**, 074107.

10 MRCC, a quantum chemical program suite written by M. Kállay, P. R. Nagy, D. Mester, Z. Rolik, G. Samu, J. Csontos, J. Csóka, P. B. Szabó, L. Gyevi-Nagy, B. Hégely, I. Ladjánszki, L. Szegedy, B. Ladóczki, K. Petrov, M. Farkas, P. D. Mezei and Á. Ganyecz. See www.mrcc.hu.

11 D. A. Tasi, T. Győri and G. Czakó, *Phys. Chem. Chem. Phys.*, 2020, **22**, 3775.

12 T. Győri and G. Czakó, *J. Chem. Theory Comput.*, 2020, **16**, 51.

13 B. J. Braams and J. M. Bowman, *Int. Rev. Phys. Chem.*, 2009, **28**, 577.

14 J. M. Bowman, G. Czakó and B. Fu, *Phys. Chem. Chem. Phys.*, 2011, **13**, 8094.

15 K. A. Brueckner, *Phys. Rev.*, 1954, **96**, 508.

16 P. Papp, V. Tajti and G. Czakó, *Chem. Phys. Lett.*, 2020, **755**, 137780.